ORGANOMETALLICS

pubs.acs.org/Organometallics Article

Tricyclic Sulfoxide−Alkene Hybrid Ligands for Chiral Rh(I) Complexes: The "Matched" Diastereomer Catalyzes Asymmetric C−C Bond Formations

Alexander Nikol, Ziyun Zhang, Ahmed Chelouan,* Laura Falivene, Luigi Cavallo, Alberto Herrera, Frank W. Heinemann, Ana Escalona, Sibylle Frieß, Alexander Grasruck, and Romano Dorta*

Cite This: https://dx.doi.org/10.1021/acs.organomet.0c00094 Read Online

ACCESS | Metrics & More | Article Recommendations | Supporting Information

ABSTRACT: Deprotonation of phenyldibenzo[*b*,*f*]tropylidene (**8**) with LDA/*t*-BuOK followed by quenching with either diastereomer of inexpensive glucose-based *t*-Bu-sulfinate (*R*)- or (*S*)-**11** affords a sulfoxide−alkene hybrid ligand as the diastereomeric pairs (S_S,S_C)-**9**/(S_S,R_C)-**10** and (R_S,R_C)-**9**/(R_S,S_C)-**10**, respectively, which via chromatographic/recrystallization may be separated into the four isomers. The optically pure diastereomeric ligands (S_S,S_C)-**9** and (S_S,R_C)-**10** react with $[RhCl(coe)_2]_2$ to form the dinuclear complexes (R_S,S_C)-**11** and (R_S,R_C)-**12**, respectively, in which the bidentate ligands coordinate the metal centers through the sulfur and alkene donor functions. These complexes catalyze the conjugate addition of arylboronic acids to cyclic Michael acceptors with enantioselectivities of up to 99% ee. DFT calculations show the preponderant influence of planar chirality of the ligand alkene function. The enantioselectivity switch observed between (R_S,S_C)-**11** and (R_S,R_C)-**12** is explained by the inverted *cis*−*trans* coordinations of the substrate molecules in catalytic steps.

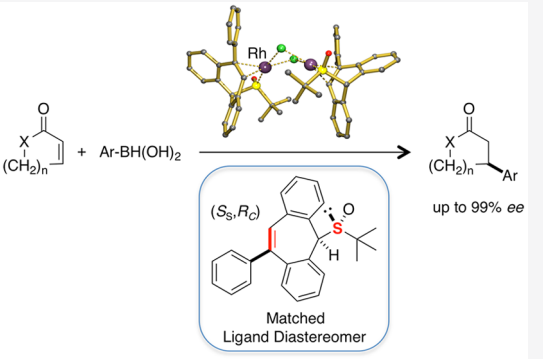

INTRODUCTION

The development of new ligand designs for chiral metal complexes is paramount for the advancement of asymmetric catalysis.[1] For some time, we have been interested in hybrid P-alkene ligands such as **1** and **2** based on the tricyclic dibenz[*b*,*f*]azepine scaffold (see Table 1).[2] The azepine−alkene function has been proven to be hemilabile,[3] a property imparting metal catalysts, even with a L/M stoichiometry of 2/1 such as $[Rh(\mathbf{1})_2][BF_4]$[4] and $[Ir(\mathbf{1})_2Cl]$,[5] high selectivity, activity, and stability. Apart from P-alkene ligands, chiral bis-alkenes,[6] bis-sulfoxides,[7] and in particular S(O)-alkene[8] hybrids have emerged as the ligands of choice for the asymmetric Hayashi−Miyaura reaction.[9] The ease of synthesis and high stability of enantiopure sulfoxides and the recent finding that polarized $R_2S^+-O^-$ ligand functions appear to induce chirality also through electrostatic effects[10] prompted us to extend the S(O)-alkene ligand architecture to tricyclic systems. Inspired by Knochel's highly effective sulfoxide−alkene **3**[11] and Liao's stereoselectivity-switching S(O)-alkenes (both planar-chiral systems),[12] we recently disclosed the planar-chiral sulfonamide **4**.[13] Since this ligand proved stereochemically stable only at specific pH values, we were interested in replacing the sulfinamido S−N bond[14] with the more robust sulfoxide S−C bond of the dibenzotropylidene analogue (i.e., replacing the N atom with a C−H moiety; see Table 1).[15] Here, we describe a simple protocol for the stereodivergent synthesis of this new class of enantiopure, tricyclic sulfoxide−alkene ligands, which

Table 1. Inspiring Chiral P-Alkene and S-Alkene Ligands and the Targeted Tricyclic Sulfoxide−Alkene

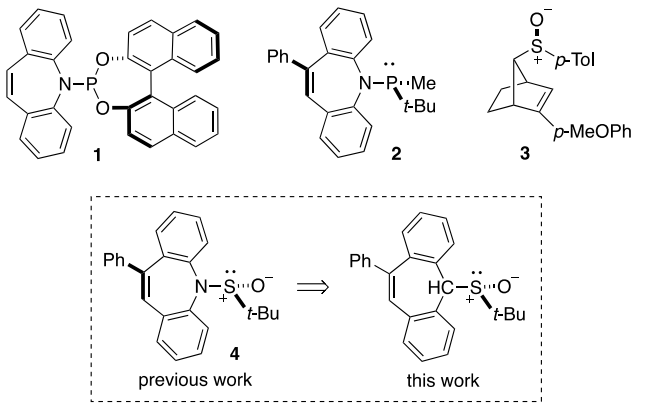

Received: February 10, 2020

are a nice bidentate fit for Rh(I). We show that the rhodium complex of the matched ligand diastereomer[16] is a highly selective catalyst for the asymmetric Hayashi–Miyaura reaction and provide mechanistic insight and a stereochemical model by DFT calculations.

RESULTS AND DISCUSSION

Exploring ways to construct the C–S bond of the sought-after sulfoxide-tropylidene analogue of **4**, we soon found out that common sulfinate electrophiles reacted cleanly only with *in situ* deprotonated phenyldibenz[*a*,*d*]tropylidene (**8**) (at C9; see Scheme 1), while the use of more straightforward Grignard or

Scheme 1. Multigram Synthesis of 8 and Its Planar-Chiral Structure in the Crystal[a]

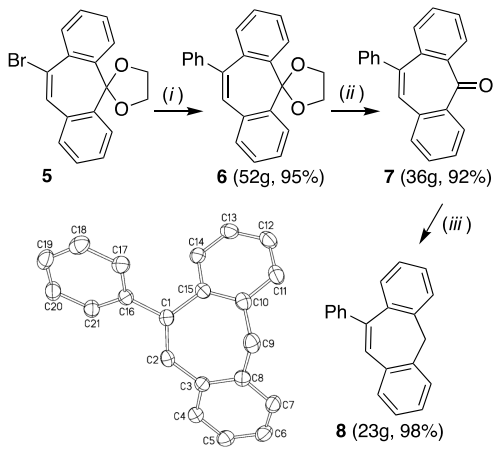

[a]Conditions: (i) $PhB(OH)_2$ (1 equiv), $Pd(PPh_3)_4$ (5 mol %), DME, reflux, 18 h; (ii) HCl, THF, reflux, 72 h; (iii) $AlCl_3$, $LiAlH_4$, Et_2O/THF, reflux, 16 h. Crystal structure of **8** (50% displacement ellipsoids; H, atoms omitted). Selected distances (Å) and angles (deg): C(1)–C(2) 1.3465(19), C(1)–C(2)–C(3) 128.71(13), C(2)–C(1)–C(15) 123.68(12), C8–C9–C10 110.97(11).

lithium nucleophiles obtained from phenyldibenz[*a*,*d*]-tropylidenyl chloride invariably led to impure products. However, the limited scalability of reported synthetic routes to **8**[17] prompted us to develop a 50 g scale Suzuki coupling of phenylboronic acid with the bromoalkene precursor **5**.[18] Deprotection and reduction of product **6** routinely yields 20 g quantities of white crystalline **8** with a high melting point. In the crystal, **8** is a planar-chiral racemate with a boat-shaped tropylidene moiety, while in solution at room temperature it inverts rapidly via a planar transition state with a DFT-calculated barrier of 13.1 kcal/mol.[19]

Before tackling the asymmetric synthesis of the ligand, we isolated its racemic form: reacting deprotonated **8** with *rac*-*t*Bu-S(O)Cl affords the diastereomeric pairs *rac*-**9** + *rac*-**10** because of the stereogenic benzyl C atom.[20] The isomers turned out to be readily separable by enantioselective HPLC (see Scheme 2), which indicated that stereochemically stable molecules should be amenable to asymmetric synthesis. Indeed, deprotonation of **8** with LDA/KO*t*Bu[21] followed by *in situ* quenching at −78 °C with the inexpensive glucose-derived sulfinate (*R*)-**11**[22] in THF gives the alkene–sulfoxides (S_S,S_C)-**9** and (S_S,R_C)-**10** in a ca. 5/3 diastereomeric mixture[23] (see Scheme 3). The diastereomers are separated by flash column chromatography/crystallization[24] and isolated on gram scales and in excellent optical purity (verified by HPLC; see Figures S4 and S5 in the Supporting

Scheme 2. Symmetric Synthesis of the *t*-Bu-Sulfoxide–Alkene Ligand Giving Rise to Diastereomeric Pairs of Enantiomers *rac*-9 + *rac*-10 in a ca. 1/1 Ratio and Their Separation by Chiral Stationary Phase HPLC[a]

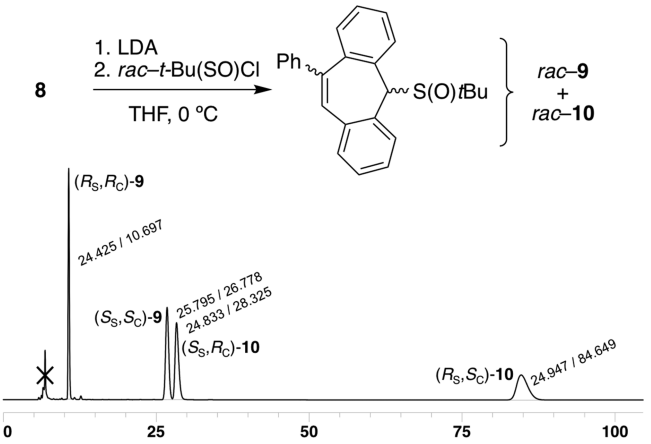

[a]The trace shows area/retention times in minutes. Absolute configurations were assigned by single-crystal XRD analysis of optically pure ligands (*vide infra* and the Supporting Information). Conditions: Daicel Chiralpak AD-H; flow rate: 0.7 mL/min; *n*-hexane/*i*-PrOH = 8/2.

Scheme 3. Stereodivergent Syntheses of the Diastereomeric S(O)-Alkenes 9 and 10

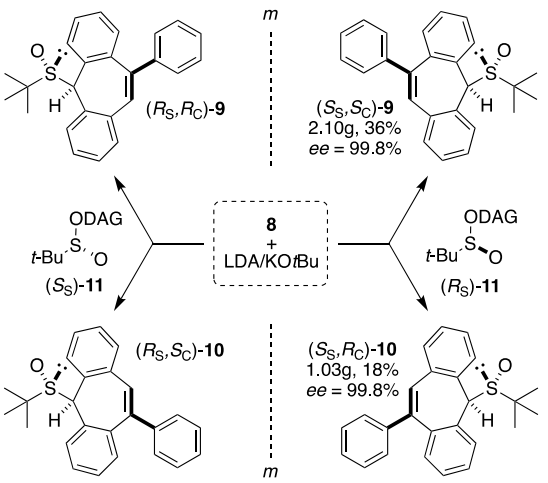

Information). (S_S,S_C)-**9** and (S_S,R_C)-**10** are best identified by the characteristic singlet resonances of the *t*-Bu groups at 1.24 and 1.19 ppm in their respective ^{1}H NMR spectra. The ligands do not epimerize in C_6D_6 solution on prolonged heating at 60 °C.

In order to gain precise structural information for unambiguous assignment of the absolute configurations of the stereocenters in **9** and **10** and for identification of the HPLC peaks in Scheme 2, single-crystal X-ray diffraction analyses were performed. The molecular structures are depicted in Figure 1 and confirm the expected *S*-configured sulfur atoms (C–S bond formation takes place with inversion of configuration) and, most importantly, reveal the absolute configurations of the carbon stereocenters, which are *S* and *R*, respectively. The stereogenic sulfur and carbon atoms are pyramidal with average bond angles of 104.6 and 110.9° for **9** and 104.5 and 110.6° for **10**, respectively. On the other hand, the phenyl-substituted atoms C9 and C8 are perfectly trigonal planar in both structures

https://dx.doi.org/10.1021/acs.organomet.0c00094
Organometallics XXXX, XXX, XXX–XXX

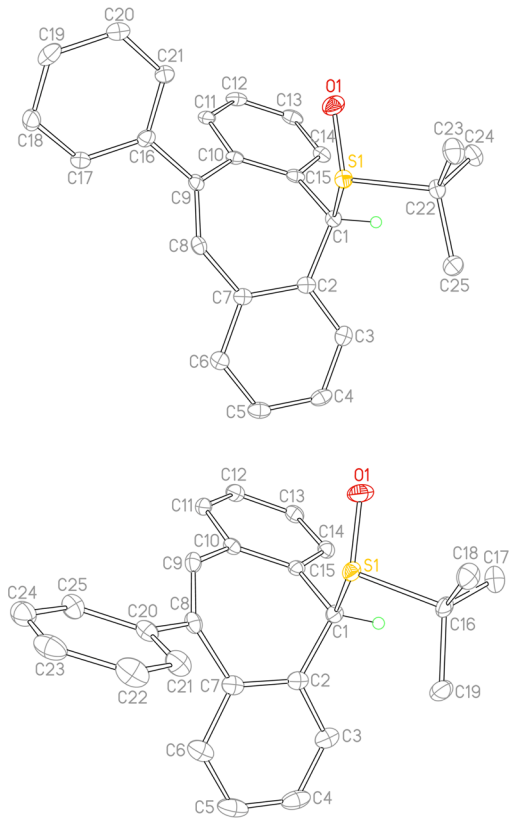

Figure 1. Molecular structures of (S_S,S_C)-**9** (top) and (S_S,R_C)-**10** (bottom) in the respective chiral crystals (50% displacement ellipsoids; H atoms are omitted except on C1). Selected distances (Å) and angles (deg): for (S_S,S_C)-**9**, S1−O1 1.4983(17), S1−C1 1.894(3), S1−C22 1.856(3), C8−C9 1.353(3), C9−C16 1.499(4), C22−S1−C1 101.82(11), O1−S1−C1 106.73(11), O1−S1−C22 105.15(11), C2−C1−S1 110.63(16), C8−C9−C16 116.6(2), C2−C1−C15 114.0(2); for (S_S,R_C)-**10**, S1−O1 1.5006(13), S1−C1 1.8714(17), S1−C16 1.8534(17), C8−C9 1.347(2), C8−C20 1.491(2), C16−S1−C1 100.32(8), O1−S1−C1 106.74(8), O1−S1−C16 106.37(8), C2−C1−S1 109.64(11), C9−C8−C20 119.46 (15), C2−C1−C15 111.5(14).

(average bond angles of 120.0°). As a proof of principle that all four stereoisomers may be accessible, the anion of **8** was also reacted with the (*S*)-**11** diastereomer of the DAG-sulfinate to afford diastereomers (R_S,R_C)-**9** and (R_S,S_C)-**10** (Scheme 3).[25] The crystal structure of (R_S,R_C)-**9** is indeed the enantiomorph of (S_S,S_C)-**9** (see Figure S7 in the Supporting Information), showing consistent stereochemistry and further confirming the HPLC peak assignment.

The coordination behavior of (S_S,S_C)-**9** and (S_S,R_C)-**10** with Rh(I) was assessed by reacting 2 equiv of the respective ligands with $[RhCl(coe)_2]_2$ (coe = cyclooctene) in benzene or toluene solution to yield dinuclear complexes (*R*,*S*)-**11** and (*R*,*R*)-**12** almost quantitatively as yellow-orange powders (Scheme 4). The complexes are soluble in CH_2Cl_2 but much less so in aromatic solvents. NMR spectra of complex **11** in CD_2Cl_2 solution show a mixture of *syn* and *anti* isomers in a 1/2 ratio, while complex **12** forms exclusively as the *anti* isomer. The perfect *anti* selectivity of ligand **10** in the synthesis of complex **12** parallels its superior enantioselectivity in catalysis (*vide infra*) and the strong diastereoselective interaction with the chiral stationary phase in HPLC separation causing a large difference in retention times (Scheme 2, *vide supra*). Single-crystal X-ray diffraction analyses of the complexes *confirm the bidentate coordination mode of the S-alkene ligands* and show square-planar coordination geometries around the chloro-bridged Rh centers (see Figures 2 and 3).[26] The butterfly-shaped Rh_2Cl_2 cores in **11** and **12** span wing angles of 120.4 and 167.5°, respectively. Exclusive *anti* coordination is observed in both crystals. In both complexes, the *trans* influences exerted by the alkene vs S-donors differ significantly: Rh−Cl distances *trans* to the S atoms are 0.06−0.08 Å longer than the corresponding bonds *trans* to the alkene donors. The bite angles of the ligands, measured between the centroids of the alkene functions and the S donors, are very similar at 93.7° in **11** (average value of two independent ligands) and 94.5° in **12**. The coordinated alkene bonds (C9−C8 1.432(9) Å and C34−C33 1.434(9) Å in **11**; C7−C8 1.429(11) Å in **12**) are ca. 0.08 Å longer than those in the respective free ligands **9** and **10** (1.353(3) and 1.347(2) Å; see Figure 1), and the C atoms bearing the phenyl substituents are slightly pyramidalized (sum of angles between C−C bonds is in the range 354.1−355.1°). These observations reflect metal to alkene π back-bonding.[27] Furthermore, the Rh−C distances to the phenyl-substituted C atoms are on average 5 pm (for **11**) and 8

Scheme 4. Synthesis of Dinuclear Rh(I) Complexes Bearing Ligands 9 and 10

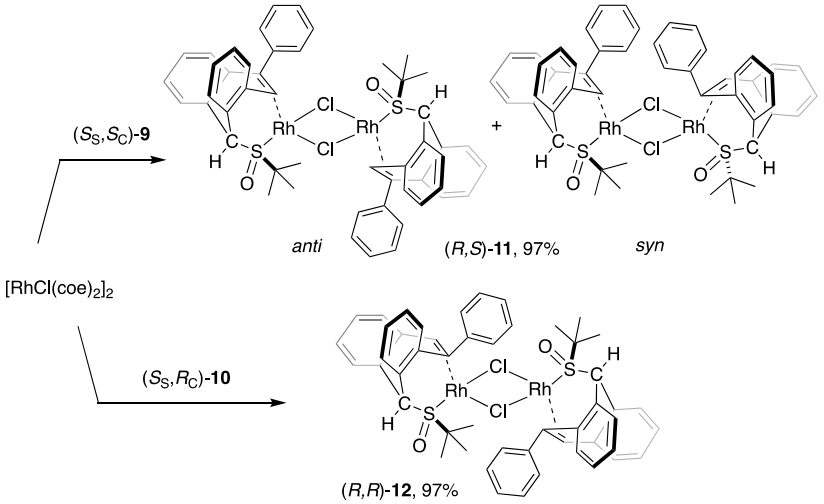

https://dx.doi.org/10.1021/acs.organomet.0c00094
Organometallics XXXX, XXX, XXX−XXX

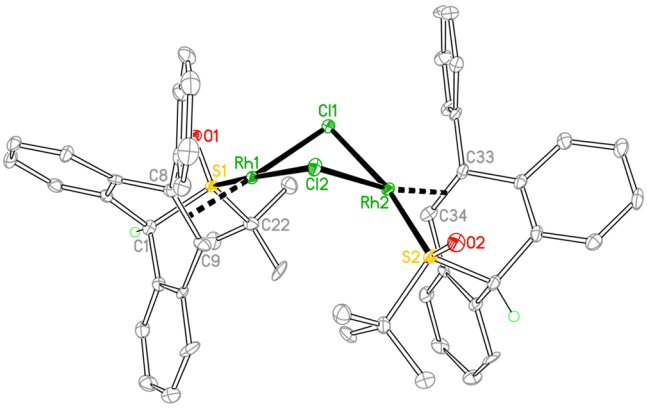

Figure 2. Molecular structure of *anti*-(*R*,*S*)-**11** in the chiral crystal (50% displacement ellipsoids; H atoms are omitted). Selected distances (Å) and angles (deg): Rh1−S1 2.1670(15), Rh1−Cl1 2.3777(15), Rh1−Cl2 2.4535(15), Rh1−C9 2.118(6), Rh1−C8 2.167(6), Rh2−Cl1 2.4414(15), Rh2−Cl2 2.3603(15), Rh2−C34 2.109(6), Rh2−C33 2.150(6), C9−C8 1.432(9), C34−C33 1.434(9), S1−O1 1.485(4), S1−C1 1.842(6), S1−C22 1.875(6).

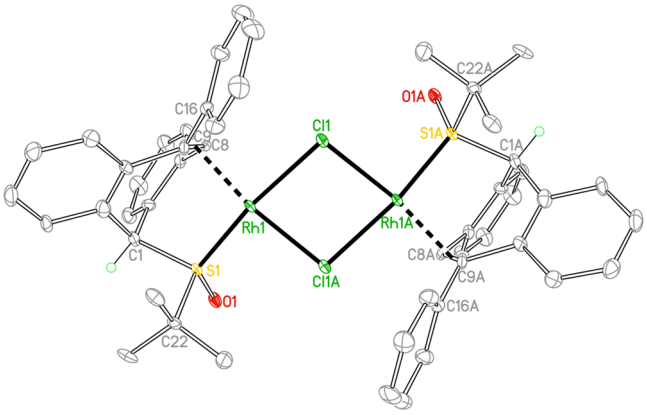

Figure 3. Molecular structure of (*R*,*R*)-**12** in the chiral crystal (50% displacement ellipsoids; H atoms are omitted). Selected distances (Å) and angles (deg): Rh1−Cl1 2.4305(16), Rh1−Cl1A 2.3723(16), Rh1−C8 2.109(7), Rh1−C9 2.192(7), Rh1−S1 2.1590(17), S1−O1 1.481(5), S1−C1 1.846(7), S1−C22 1.880(7), C8−C9 1.429(11), C9−C16 1.482(10), Rh1A−Cl1−Rh1 98.68(6), S1−Rh1−Cl1A 92.56(6), C8−Rh1−Cl1 89.2(2), C9−Rh1−Cl1 93.96(19).

pm (for **12**) longer than the distances to the unsubstituted C atoms.

With well-characterized optically pure complexes **11** and **12** in hand, their performance in asymmetric catalysis was benchmarked in the Hayashi−Miyaura conjugate addition of arylboronic acids to enones (see Table 1). Standard reaction conditions consisted of a 1,4-dioxane/H_2O solvent system, Cs_2CO_3 additive, 40 °C, and a 3 mol % catalyst loading to ensure complete conversions (>95% isolated yields; optimization of catalyst activity was not a priority in this study).[28] Even though catalysts (*R*,*S*)-**11** and (*R*,*R*)-**12** bear identically configured sulfur donor atoms, entries 1 and 2, 4 and 5, and 14 and 15 reveal a preference for opposite configurations in the addition products. Clearly, the opposite planar chirality of the coordinated alkene functions that characterizes the two complexes is the overwhelming factor that determines the stereochemical outcome in these reactions. Additionally, complex (*R*,*R*)-**12** displays vastly superior enantioselectivity, which *identifies ligand **10** as the "matched" ligand diastereomer* with the two stereocenters working in synergy. The observation that enantioselection is predominantly governed by the planar chirality of the coordinated alkene function (and not the chirality of the S donor) has previously been made by Knochel and co-workers,[11] by Liao and co-workers,[12] and by ourselves[13] with similar S(O)-alkene ligand systems. In general, while catalyst **12** gives satisfactory enantioselectivities in additions of aryl nucleophiles to cyclohexenone, it compares favorably with the best S(O)-alkene ligands for additions to cyclopentenone and dihydropyranone.

In order to get a precise mechanistic picture of this reaction and to rationalize the disparate enantioselectivities observed for catalysts **11** and **12** (entries 1 and 2, 4 and 5, and 14 and 15 in Table 2), the prototypical reaction of cyclohexenone **14a** with phenylboronic acid **15a** was investigated by DFT calculations. The first step of the catalytic cycle is well established and consists of transmetalation of the phenyl nucleophile from the boronic acid to the metal, affording the nucleophile−rhodium intermediate (**A** in Figure 4).[29] With this species as the starting point, set as the zero point energy, the cyclohexenone electrophile presents its *re* or *si* face to the Rh−Ph bond via a [2 + 2] transition state, leading to the *R*- or *S*-configured ketone, respectively, after hydrolysis. We focused on the coordination/insertion step affecting the enantioselectivity of the reaction. The energy profiles for **11** and **12** in Figure 4 show that phenyl coordination *trans* to the π-accepting alkene donor is favored in both cases (**11-A** and **12-A**), while the alternative species **A1** with the phenyl groups lying *trans* to the sulfoxide ligand are approximately 7 kcal/mol higher in energy. The approach of the enone to **A** occurs *trans* to the sulfoxide ligand via transition state **A-B** with energy barriers of 8.8 and 5.0 kcal/mol for **11** and **12**, respectively. From intermediate **B** the two catalysts behave differently: in the case of **11**, the system prefers first to isomerize to the lower energy intermediate **B1** with the phenyl *cis* to the alkene ligand, thereby gaining 5.0 kcal/mol, and then to insert via transition state **B1-C**, rather than to insert directly from **B**. In fact, both the **B** → **B1** *cis*/*trans* isomerization barrier (12.6 kcal/mol calculated from **A**) and the following insertion barriers (16.5 and 19.0 kcal/mol leading to the *R*- and *S*-configured products, respectively), are lower than the direct insertion barriers from **B** (18.4 and 20.7 kcal/mol for *R*- and *S*-configured products, respectively), due to a strongly distorted square planar geometry of the corresponding transition states ascribed to steric repulsions between the ligand phenyl ring and the phenyl nucleophile. The free energy difference between the two competing transition states of 2.5 kcal/mol in favor of pro-(*R*) **B1-C** for **11** implies predominant insertion of the *re* face of the enone to the *R* product, in agreement with experiments. In the case of catalyst **12**, on the contrary, the favored insertion step occurs from **12-B** with the phenyl *cis* to the sulfoxide ligand and with energy barriers of 14.9 and 10.6 kcal/mol for the *R*- and *S*-configured products, respectively. The free energy difference between the two competing transition states of 4.3 kcal/mol in favor of pro-(*S*) **B-C** explains the observed high enantioselectivity for the *S* product. The alternative pathway with the phenyl group *trans* to the sulfoxide ligand was ruled out because it has higher energy barriers of 15.5 and 17.4 kcal/mol for *R*- and *S*-configured products, respectively (see Figure S40 in the Supporting Information for a detailed discussion). It is worth noting that the opposite *cis*/*trans* arrangements of the phenyl and enone substrate molecules in the favored intermediates and transition states for **11** and **12** are the result of steric effects of the opposite planar chirality of the phenyl-alkene ligand function.

https://dx.doi.org/10.1021/acs.organomet.0c00094
Organometallics XXXX, XXX, XXX−XXX

Table 2. Catalytic Performance of Complexes 11 and 12 in the Hayashi–Miyaura Conjugate Addition Reaction

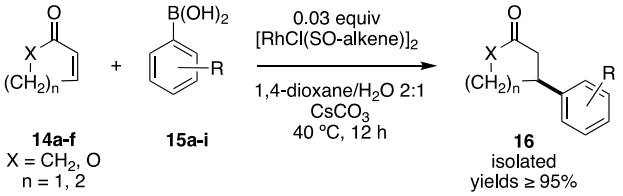

14a-f X = CH_2, O; n = 1, 2 + **15a-i** → **16** isolated yields ≥ 95%

entry	catalyst	enone	arylboronic acid, R [a]	product	*ee* (%) [b]	major isomer [c]
1	(*R*S,*S*C)-**11**	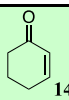 **14a**	H (**15a**)	**16aa**	50	(*R*)
2	(*R*S,*S*C)-**12**	**14a**	**15a**	**16aa**	93	(*S*)
3[d]	(*R*S,*R*C)-**12**	**14a**	4-CH_3 (**15b**)	**16ab**	97	(*S*)
4	(*R*S,*R*C)-**11**	**14a**	4-*t*Bu (**15c**)	**16ac**	39	(*R*)
5	(*R*S,*R*C)-**12**	**14a**	4-*t*Bu (**15c**)	**16ac**	95	(*S*)
6	(*R*S,*R*C)-**12**	**14a**	4-F (**15d**)	**16ad**	89	(*S*) [e]
7	(*R*S,*R*C)-**12**	**14a**	4-CH_3O (**15e**)	**16ae**	92	(*S*) [e]
8	(*R*S,*R*C)-**12**	**14a**	3-CH_3O (**15f**)	**16af**	90	(*S*) [e]
9	(*R*S,*R*C)-**12**	**14a**	2-CH_3O (**15g**)	**16ag**	82	(*S*) [e]
10	(*R*S,*R*C)-**12**	**14a**	1-naph (**15i**)	**16ai**	85	(*S*) [e]
11	(*R*S,*R*C)-**12**	**14a**	2-naph (**15h**)	**16ah**	90	(*S*)
12	(*R*S,*R*C)-**12**	 **14b**	H (**15a**)	**16ba**	96	(*S*)
13	(*R*S,*R*C)-**12**	**14b**	4-CH_3 (**15b**)	**16bb**	95	(*S*)
14	(*R*S,*R*C)-**11**	**14b**	4-*t*Bu (**15c**)	**16bc**	48	(*R*)
15	(*R*S,*S*C)-**12**	**14b**	4-*t*Bu (**15c**)	**16bc**	97	(*S*)
16	(*R*S,*R*C)-**12**	**14b**	4-F (**15d**)	**16bd**	94	(*S*) [e]
17	(*R*S,*R*C)-**12**	**14b**	4-CH_3O (**15e**)	**16be**	95	(*S*)
18	(*R*S,*R*C)-**12**	**14b**	3-CH_3O (**15f**)	**16bf**	96	(*S*) [e]
19	(*R*S,*R*C)-**12**	**14b**	2-CH_3O (**15g**)	**16bg**	99	(*S*) [e]
20	(*R*S,*R*C)-**12**	**14b**	1-naph (**15i**)	**16bi**	97	(*S*)
21	(*R*S,*R*C)-**12**	**14b**	2-naph (**15h**)	**16bh**	94	(*S*)
22	(*R*S,*R*C)-**12**	 **14c**	H (**15a**)	**16ca**	95	(*S*) [e]
23	(*R*S,*R*C)-**12**	**14c**	4-CH_3 (**15b**)	**16cb**	95	(*S*)
24	(*R*S,*R*C)-**12**	**14c**	4-*t*Bu (**15c**)	**16cc**	98	(*S*) [e]
25	(*R*S,*R*C)-**12**	**14c**	4-F (**15d**)	**16cd**	94	(*S*) [e]
26	(*R*S,*R*C)-**12**	**14c**	4-CH_3O (**15e**)	**16ce**	94	(*S*) [e]
27	(*R*S,*R*C)-**12**	**14c**	3-CH_3O (**15f**)	**16cf**	97	(*S*) [e]
28	(*R*S,*R*C)-**12**	**14c**	2-CH_3O (**15g**)	**16cg**	97	(*S*)
29	(*R*S,*R*C)-**12**	**14c**	1-naph (**15i**)	**16ci**	96	(*S*) [e]
30	(*R*S,*R*C)-**12**	**14c**	2-naph (**15h**)	**16ch**	94	(*S*)

[a]Commercial arylboronic acids were used as received. [b]Determined by enantioselective HPLC (see the Supporting Information). [c]Absolute configurations are assigned by comparison with reported data. [d]Toluene used instead of dioxane. [e]Assumed configurations.

Thus, the theoretical comparison between the two catalysts is in nice agreement with experiments (even though the respective absolute $\Delta\Delta G^{\ddagger}_{resi}$ *values are somehow overestimated by the calculations): the enantioselectivity of* **12** *in favor of the S-configured insertion product is almost 2 kcal/mol higher than that displayed by* **11** *in favor of the R product.*

An analysis of the favored transition state geometries **11** pro-(*R*) **B1-C** and **12** pro-(*S*) **B-C** in Figure 5 (top left and bottom right structures) highlights the cyclohexenone ring carbons placed in a rather open space, *anti* to the S-*t*-Bu and the alkenyl phenyl groups, respectively. In contrast, the disfavored transition states **11** pro-(*S*) **B1-C** and **12** pro-(*R*) **B-C** are destabilized by steric repulsion between the cyclohexenone ring and ligand donor functions. In **11**, enantiodifferentiation of the cyclohexenone ring occurs by interaction with only one carbon atom of the *cis*-positioned S-*t*-Bu group, with the planar-chiral phenyl–alkene ligand function *trans* to the enone having no influence (see Figure 5, top right). In **12**, the cyclohexenone ring is *cis* to the phenyl–alkene ligand and, thus, this function becomes the determining steric factor with multiple steric clashes at short distances between the cyclohexenone and the ligand phenyl group (see Figure 5, bottom left).

Figure 6 schematically summarizes the differences between the two catalysts in the enantioselective insertion step[30] and shows the steric maps around Rh calculated by the SambVca software.[31] The maps allow rationalizing the results discussed above as a function of the symmetry of the catalytic pocket. In both cases, the phenyl group of the alkene donor of the ligand

https://dx.doi.org/10.1021/acs.organomet.0c00094
Organometallics XXXX, XXX, XXX–XXX

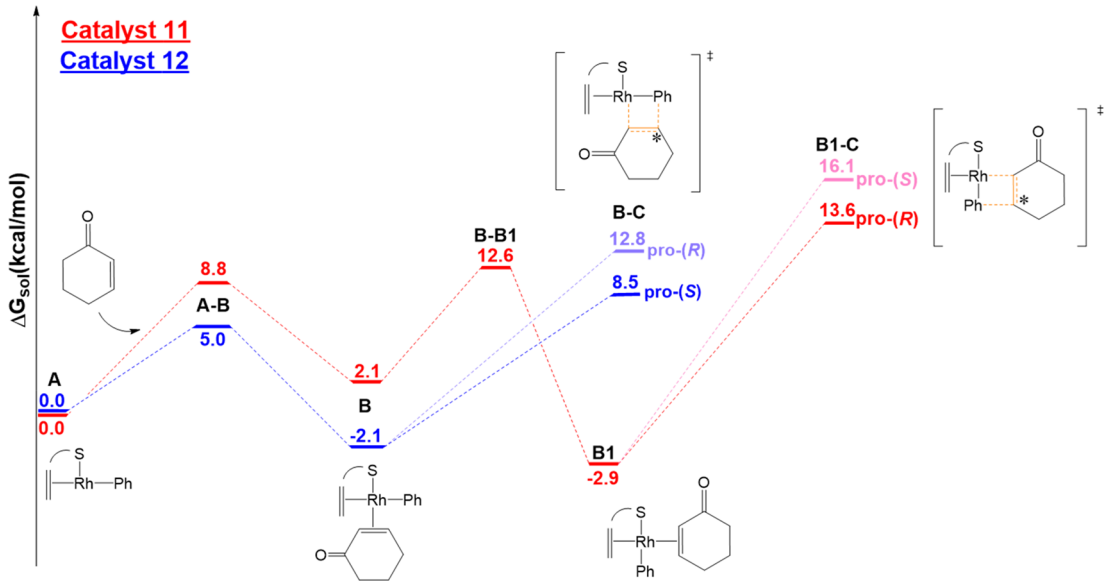

Figure 4. Energy profiles for the insertion step of the Hayashi−Miyaura conjugate addition of cyclohexanone and phenylboronic acid in the presence of **11** (in blue) and **12** (in red). Free energies are given in kcal/mol in 1,4-dioxane solvent.

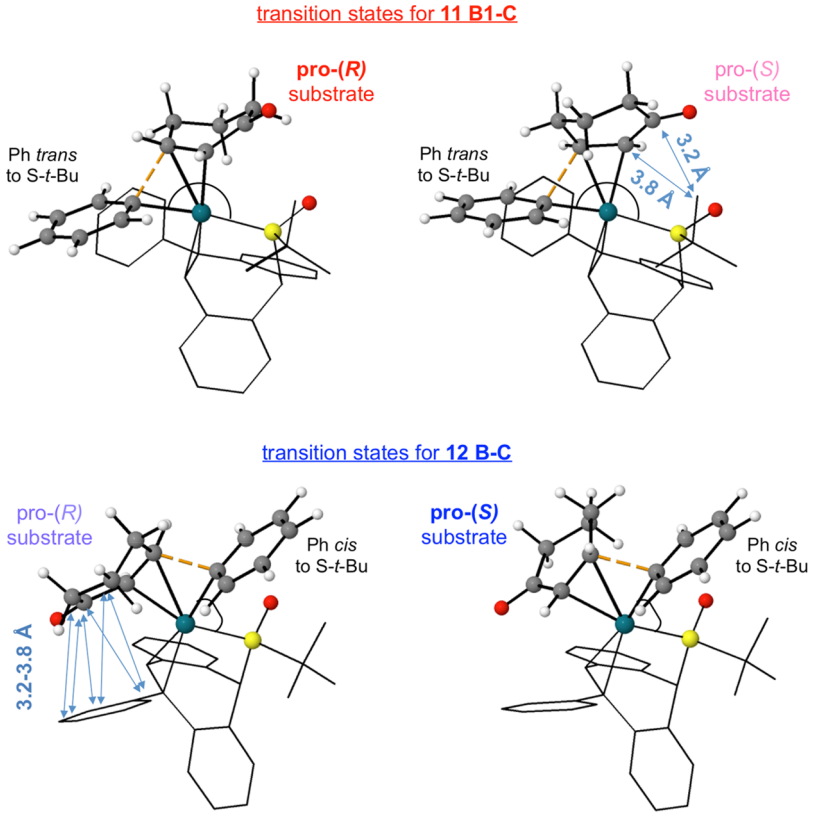

Figure 5. Optimized geometries of the insertion transition states with **11** (top) and **12** (bottom).

causes more encumbrance (northwest (NW) and southwest (SW) quadrants for **11** and **12**, respectively) in comparison to the S-*t*-Bu donor (orange contours in the southeast quadrants (SE) denote one out of three methyl groups, which in solution rotate freely). The coordination environment for **11** (left diagram) is quasi C_2 symmetric, while that for **12** (right diagram) is quasi C_s symmetric, with both ligand donors obstructing the south quadrants.[32] As a consequence, with **12**, the pro-(*S*) enantiospecific coordination of the enone is more forced than with **11** in order to avoid the clash of the cyclohexanone ring with the highly hindered alkene ligand in the SW quadrant (compare the substrate schemes in Figure 6c and the hindered quadrants in the maps).

CONCLUSION

The stereoselective, divergent synthesis of the four possible isomers of a new tricyclic sulfoxide−alkene hybrid ligand has been demonstrated. Diastereomers **9** and **10** are excellent

https://dx.doi.org/10.1021/acs.organomet.0c00094
Organometallics XXXX, XXX, XXX−XXX

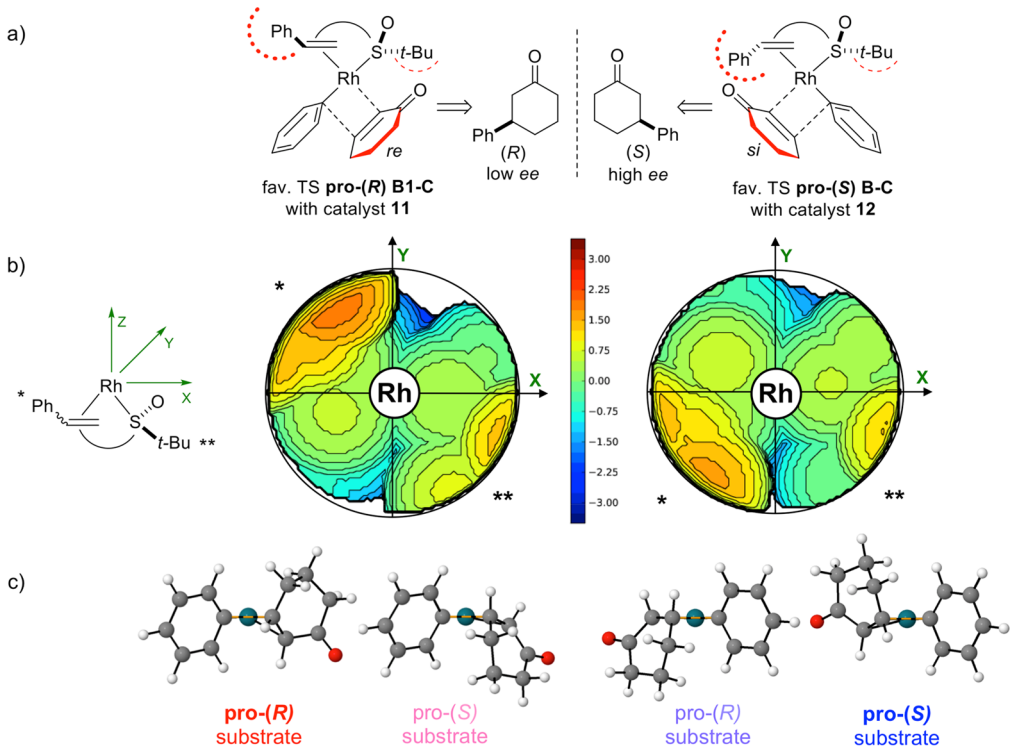

Figure 6. (a) Stereochemical model (top view) for the prediction of the sense of addition of **14a** to **13a** when ligand (S_S,S_C)-**9** (left) or ligand (S_S,R_C)-**10** (right) is used. (b) Steric maps of the respective Rh(I) complexes (R_S,S_C)-**11** and (R_S,R_C)-**12** from crystallographic data. The steric maps are viewed down the *z* axis; the orientation of the complexes is indicated on the left. Rh atoms, H atoms, and secondary ligands were excluded in the calculations. Sphere radii are 3.5 Å, and Bondi radii are scaled at 1.17. The isocontour scheme, in Å, is shown in the middle. Red and blue zones indicate the more and less hindered zones in the catalytic pocket, respectively. (c) Ball-and-stick representation of the *R*- and *S*-configured product formations as in the favored transition states reported in Figure 5.

bidentate ligands for Rh(I), and the respective isolated complexes **11** and **12** catalyze the asymmetric Hayashi−Miyaura reaction. The superior enantioselectivity displayed by complex **12** bearing the "matched" ligand diastereomer (S_S,R_C)-**10** and the reversal and lowering of chiral induction observed with complex **11** bearing the ligand diastereomer (S_S,S_C)-**9** (with a sulfur donor of chirality identical with that of the ligand (S_S,R_C)-**10**) is explained by DFT calculations. **11** and **12** promote similar catalytic cycles with enantioselection occurring in the insertion step, with the difference that the favored insertion transition states in **11** and **12** present opposite *cis*/*trans* arrangements of the enone/phenyl substrates with respect to the ligand sulfur and alkene donors. We conclude that in electronically dissymmetric S-alkene ligand systems sterics *and* electronics (leading to *trans* effects in the square-planar Rh(I) intermediates) are operative in the Hayashi−Miyaura reaction and that ligand geometries that create quasi C_2 coordination environments on Rh should be avoided. This is in contrast to well-established electronically and C_2-symmetric bis-alkene, bis-sulfoxide, and bis-phosphine systems.[33] Finally, the remarkable enantioselectivities achieved with ligand **10** in its prototype version for the Hayashi−Miyaura reaction bodes well for other applications, not least because the simple synthetic protocol for this ligand is amenable to modification for steric and electronic optimization at both donor functions.

EXPERIMENTAL SECTION

Experiments involving sensitive compounds were carried out under anaerobic and anhydrous conditions, using standard Schlenk and inert-gas glovebox techniques. Technical grade EtOAc and hexanes for flash column chromatography were purified by rotary evaporation. THF, Et_2O, and benzene were distilled from purple Na/Ph_2CO solutions, toluene was distilled from Na, pentane, C_6D_6, and THF-d_8 were distilled from Na_2K alloy, CH_3CN, CH_2Cl_2, and CD_2Cl_2 were distilled from CaH_2, and NEt_3 and 1,4-dioxane were distilled from K. CD_3CN and $CDCl_3$ were degassed with three freeze−pump−thaw cycles and then kept in a glovebox over activated molecular sieves (3 and 4 Å, respectively). Arylboronic acids, LDA (purchased from Sigma-Aldrich), and DME (from TCI) were used as received. **5**,[18] (R_S)- and (S_S)-1,2:5,6-di-*O*-isopropylidene-*α*-D-glucofuranosyl *tert*-butylsulfinate ((*R*)-**11** and (*S*)-**11**),[34] PhLi,[35] $[RhCl(coe)_2]_2$,[36] and *tert*-butanesulfinyl chloride[37] were prepared according to published procedures. $LiAlH_4$ (Sigma-Aldrich) was extracted in Et_2O and used as a snow-white crystalline powder. Elemental analyses (EA) were performed on a Euro EA 3000 analyzer, and air-sensitive samples were handled and prepared in a glovebox. NMR spectra were recorded on Jeol EX 270, ECP 400, and ECX 400 instruments operating at 269.71, 399.78, and 400.18 MHz for ^{1}H, at 67.82, 100.52, and 100.62 MHz for ^{13}C, and at 161.83 and 162.00 MHz for ^{31}P, respectively. Chemical shifts are given in ppm and are reported relative to residual solvent peaks as secondary standards.[38] Jeol's *Delta NMR Processing and Control Software* was used to process and visualize the NMR data.[39] HPLC was performed on a Shimadzu LC10 series instrument.

10-Phenyl-5,5-ethylenedioxy-*5H*-dibenzo[*a*,*d*]cycloheptene (6). **5** (55.0 g, 168 mmol), phenylboronic acid (24.4 g, 197 mmol), $Pd(PPh_3)_4$ (5.58 g, 4.80 mmol), degassed DME (1.38 L), and Na_2CO_3 (26.2 g, 247 mmol, 2 M in H_2O, 123.75 mL) were charged into a Schlenk vessel, and the reaction mixture was heated to reflux for 40 h. After the mixture was cooled to room temperature, CH_2Cl_2 (500 mL) and water (300 mL) were added. The organic phase was separated and the aqueous phase extracted with methylene chloride (3 × 150 mL). The combined organic phases were dried over anhydrous Na_2SO_4, and evaporation of the solvent provided solid crude **5**, which was slurried in pentane (500 mL), filtered, and washed with additional pentane (3 × 150 mL) to yield a yellow solid (52 g, 95%). Mp: 145 °C. Anal. Found:

https://dx.doi.org/10.1021/acs.organomet.0c00094
Organometallics XXXX, XXX, XXX−XXX

C, 84.86; H, 5.60. Calcd for $C_{23}H_{18}O_2$: C, 84.64; H, 5.56. ^{1}H NMR (400 MHz, $CDCl_3$): δ 7.92−7.86 (m, 2H, Ar*H*), 7.52−7.17 (m, 12H, Ar*H*), 4.25 (t, $^3J_{H,H}$ = 8.0 Hz, 2H, OCH_2R), 3.84−3.74 (m, 2H, OCH_2R) ppm. ^{13}C NMR (151 MHz, $CDCl_3$): δ 144.2, 143.4, 140.3, 139.3, 134.8, 133.4, 130.3, 129.5, 129.4, 129.1, 128.3, 128.1, 127.5, 127.3, 127.1, 123.5, 123.3, 106.5, 64.8, 64.2 ppm.

10-Phenyl-5*H*-dibenzo[*a,d*]cyclohepten-5-one (7). Aqueous HCl (0.56 L, 6.0M, 3.4 mol) was added to a solution of **6** (46.0 g, 141 mmol) in THF (500 mL) and the mixture refluxed for 3 days. After the mixture was warmed to RT, 1.0 M NaOH was added until pH >7. The phases were separated, and the aqueous phase was extracted three times with EtOAc (350 mL). The combined organic phases were dried over anhydrous Na_2SO_4. The solvent was removed *in vacuo*. The crude liquid was distilled to remove glycol, the resulting solid was dissolved in EtOH (200 mL), and the suspension was heated to reflux. After 30 min, the mixture was filtered over Celite 545 (hot filtration). The orange solution was evaporated until crystals formed. To favor further crystallization, the suspension was chilled in the refrigerator to yield the product **5** (36.0 g, 92%). Mp: 120 °C. Anal. Found: C, 89.11; H, 4.89. Calcd for $C_{21}H_{14}O$: C, 89.34; H, 5.00. ^{1}H NMR (270 MHz, $CDCl_3$): δ 8.02−7.98 (m, 2H, Ar*H*), 7.61−7.38 (m, 9H, Ar*H*), 7.24−7.17 (m, 2H, Ar*H*) ppm. ^{13}C NMR (151 MHz, $CDCl_3$): δ 195.7, 144.1, 142.8, 141.1, 139.3, 135.6, 134.4, 131.6, 131.1, 130.7, 130.33, 130.28, 129.38, 128.92, 128.69, 128.48, 128.45, 128.39, 127.72 ppm.

10-Phenyl-5*H*-dibenzo[*a,d*]cycloheptene (8).[40] A solution of $AlCl_3$ (11.9 g, 89.5 mmol) in Et_2O (140 mL) was added to a solution of $LiAlH_4$ (3.39 g, 89.5 mmol) in Et_2O (140 mL). The resulting suspension was stirred for 15 min at RT, followed by cooling to 0 °C. Then a solution of **7** (25.0 g, 88.6 mmol) in THF (115 mL) was added dropwise over 20 min and the mixture heated to reflux overnight. The resulting yellowish suspension was cooled to 0 °C and quenched with water (80 mL). The aqueous layer was separated and extracted with Et_2O (3 × 200 mL). The combined organic phases were washed with water (3 × 200 mL), dried over Na_2SO_4, and evaporated *in vacuo* (23.3 g, 98%). Mp: 117 °C. Anal. Found: C, 93.69; H, 5.93. Calcd for $C_{21}H_{16}$: C, 93.99; H, 6.01. ^{1}H NMR (270 MHz, $CDCl_3$): δ 7.48−7.31 (m, 11H, Ar*H*), 7.18−6.98 (m, 2H, Ar*H*), 3.77 (s, 2H, RCH_2R^1) ppm. ^{13}C NMR (101 MHz, $CDCl_3$): δ 144.1, 143.6, 140.2, 139.3, 136.4, 135.3, 129.9, 129.5, 129.2, 128.6, 128.3, 128.1, 127.4, 127.3, 127.1, 125.9, 125.6, 41.5 ppm.

***rac*-5-*tert*-Butylsulfinyl-10-phenyl-5*H*-dibenzo[*a,d*]cycloheptene (*rac*-9 + *rac*-10).** LDA (321 mg, 3.00 mmol) in THF (10 mL) was added dropwise to a stirred solution of **8** (400 mg, 1.50 mmol) in THF (15 mL). After the reaction mixture was stirred overnight, *rac*-2-methylpropane-2-sulfinic chloride (211 mg, 1.50 mmol) in THF (30 mL) was added. Stirring was continued for 4 h, and then the solvent was removed *in vacuo*, the crude product purified by FLASH column chromatography (EtOAc), and the resulting yellow oil washed and slurried with pentane (75 mg, 13%). HPLC (Daicel Chiralpak AD-H column, hexane/*i*-PrOH 8/2, 0.7 mLmin^{-1}): t_{R1} = 10.70 min, t_{R2} = 26.78 min, t_{R3} = 28.33 min, t_{R4} = 84.65 min.

5-((*S*)-*tert*-Butylsulfinyl)-10-phenyl-5*H*-dibenzo[*a,d*]cycloheptene ((*S*$_S$,*S*$_C$)-9 and (*S*$_S$,*R*$_C$)-10). To a solution of **8** (5.00 g, 18.6 mmol) in THF (80 mL) at −78 °C under Ar was added a solution of LDA (2.00 g, 18.7 mmol) in THF (25 mL) slowly via a syringe in one portion, followed by slow addition of a solution of *t*-BuOK (2.09 g, 18.7 mmol) in THF (25 mL). The reaction mixture was stirred at −78 °C for 4 h. The reaction mixture was transferred via cannula to a solution of (*R*)-**11** (5.65 g, 15.5 mmol) in THF (100 mL) at −78 °C. The reaction mixture was stirred at −78 °C for 3 h and was slowly warmed to RT with stirring overnight. After the reaction was quenched with aqueous NH_4Cl (75 mL, saturated), EtOAc (125 mL) was added. The aqueous phase was extracted with EtOAc (3 × 60 mL). The combined organic phases were washed with brine (60 mL) and dried over Na_2SO_4. The solvent was removed *in vacuo* to afford 4.25 g of the crude diastreoisomeric mixture, which was separated by column chromatography (hexane/AcOEt 2/1) to give (*S*$_S$,*S*$_C$)-**9** (2.65 g, 46%, ee 95%) and (*S*$_S$,*R*$_C$)-**10** (1.59 g, 28%, ee 80%) as white solids. Recrystallization of (*S*$_S$,*S*$_C$)-**9** by layering a saturated and filtered THF solution with pentane affords material with ee > 99.5% (2.10 g, 36%). Mp: 143 °C. $[\alpha]_D^{25}$ = −165° (*c* = 1.0, CH_2Cl_2). Anal. Found: C, 80.23; H, 6.50; S, 8.31. Calcd for $C_{25}H_{24}OS$: C, 80.61; H, 6.49; S, 8.61. ^{1}H NMR (600 MHz, $CDCl_3$): δ 7.67 (d, $J_{H,H}$ = 6.0 Hz, 2H, Ar*H*), 7.53−7.26 (m, 9 H, Ar*H*), 7.24 (m, 2H, Ar*H*), 7.16 (d, $J_{H,H}$ = 6.0 Hz, 1H, Ar*H*), 5.27 (s, 1H, S−C*H*R$_2$), 1.24 (s, 9H, C(CH_3)$_3$) ppm. ^{13}C NMR (151 MHz, $CDCl_3$): δ 145.5, 144.2, 137.5, 136.6, 136.0, 135.4, 130.8, 130.7, 129.9, 129.7, 129.6, 129.3, 129.2, 128.5, 128.4, 127.9, 127.8, 127.6, 71.6, 55.7, 23.6 ppm. HPLC (Daicel Chiralpak AD-H column, hexane/*i*PrOH 9:1, 0.7 mLmin^{-1}): t_{R2} = 23.34 min (major). Recrystallization of (*S*$_S$,*R*$_C$)-**10** by layering a saturated and filtered EtOAc solution with hexane affords material with ee > 99.5% (1.03 g, 18%). Mp: 136 °C. $[\alpha]_D^{25}$ = −20.6° (*c* = 1.0, CH_2Cl_2). Anal. Found: C, 80.76; H, 6.48; S, 8.49. Calcd for $C_{25}H_{24}OS$: C, 80.61; H, 6.49; S, 8.61. ^{1}H NMR (600 MHz, $CDCl_3$): δ 7.42−7.26 (m, 12H, Ar*H*), 7.14−7.08 (m, 2H, Ar*H*), 5.16 (s, 1H, S-C*H*R$_2$), 1.19 (s, 9H, C(CH_3)$_3$) ppm .^{13}C NMR (151 MHz, $CDCl_3$): δ 143.8, 142.8, 137.2, 136.6, 135.8, 135.3, 131.8, 131.0, 130.9, 129.9, 129.3, 129.2, 129.0, 128.7, 128.5, 128.2, 127.8, 127.6, 70.8, 55.5, 23.8 ppm. HPLC (Daicel Chiralpak AD-H column, hexane/*i*PrOH 8/2, 0.7 mLmin^{-1}): t_{R1} = 26.45 min (major).

5-(*R*$_S$)-*tert*-butylsulfinyl-10-phenyl-5*H*-dibenzo[*a,d*]-cycloheptene ((*R*$_S$,*R*$_C$)-9 + (*R*$_S$,*S*$_C$)-10).[25] A solution of LDA (883 mg, 8.24 mmol) in THF (10 mL) was added slowly via syringe to a stirred solution of **8** (2.21 g, 8.24 mmol) in THF (40 mL) at −78 °C, followed by slow addition of a solution of *t*-BuOK (925 mg, 8.24 mmol) in THF (10 mL). The reaction mixture was stirred at −78 °C for 4 h and then transferred via cannula to a solution of (*S*)-**11** (2.50 g, 6.86 mmol) in THF (20 mL) at −78 °C. The reaction mixture was stirred at −78 °C and monitored by TLC (hexane/diethyl ether 1/1). Once the reaction was completed, it was quenched with saturated aqueous NH_4Cl (75 mL). The aqueous phase was separated and extracted with EtOAc (3 × 60 mL). The combined organic phases were washed with brine (60 mL) and dried over Na_2SO_4, and the volatiles were evaporated *in vacuo* to give a crude diastreoisomeric mixture (4.25 g, 74%, dr 5/3). This mixture was separated by column chromatography (hexane/AcOEt 2/1) and each of the diastereomers recrystallized by layering a saturated and filtered THF solution with pentane to yield (*R*$_S$,*R*$_C$)-**9** (1.22 g, 48%, ee = 89%) and (*R*$_S$,*S*$_C$)-**10** (0.62 g, 24%, ee = 80%) as white solids.

Data for (*R*$_S$,*R*$_C$)-**9** are as follows. HPLC (Daicel Chiralpak AD-H column, hexane/*i*PrOH 8/2, 0.7 mL min^{-1}): t_R = 7.45 min (major), t_R = 20.81 min (minor). Anal. Found: C, 80.74; H, 6.48; S, 8.28. Calcd for $C_{25}H_{24}OS$: C, 80.61; H, 6.49; S, 8.61. ^{1}H NMR (600 MHz, $CDCl_3$): δ 7.54 (d, $J_{H,H}$ = 7.34 Hz, 2H, Ar*H*), 7.40−7.20 (m, 9H, Ar*H*), 7.13 (m, 2H, Ar*H*), 7.02 (d, $J_{H,H}$ = 7.7 Hz, 1H), 5.14 (s, 1H, S−C*H*R$_2$), 1.15 (s, 9H, C(CH_3)$_3$) ppm. ^{13}C NMR (151 MHz, $CDCl_3$): δ 145.341, 144.12, 137.43, 136.46, 135.83, 130.72, 130.66, 129.74, 129.50, 129.23, 129.09, 128.34, 127.67, 127.48, 127.74, 71.49, 55.55, 23.42 ppm.

Data for (*R*$_S$,*S*$_C$)-**10** are as follows. HPLC (Daicel Chiralpak AD-H column, hexane/*i*PrOH 8/2, 0.7 mL min^{-1}): t_R = 22.32 min (minor), t_R = 69.76 min (major). ^{1}H NMR (400 MHz, $CDCl_3$): δ, 7.47−7.31 (m, 12H, Ar*H*), 7.31−7.15 (m, 2H, Ar*H*), 5.22 (s, 1H, S−C*H*R$_2$), 1.24 (s, 9H, C(CH_3)$_3$) ppm. ^{13}C NMR (151 MHz, $CDCl_3$): δ 145.5, 144.2, 143.8, 142.8, 137.5, 137.2, 136.5, 135.9, 135.8, 135.4, 135.3, 131.8, 131.0, 130.9, 130.8, 129.9, 129.7, 129.6, 129.3, 129.3, 129.2, 129.2, 129.0, 128.7, 128.5, 128.5, 128.2, 127.9, 127.8, 127.8, 127.6, 127.6, 71.6, 70.7, 55.7, 55.5, 23.8, 23.5 ppm.

[((*S*$_S$,*S*$_C$)-9)RhCl]$_2$ ((*R,S*)-11). A solution of (*S*$_S$,*S*$_C$)-**9** (286 mg, 0.766 mmol) in benzene (2.0 mL) was added dropwise to a stirred solution of $[RhCl(COE)_2]_2$ (275 mg, 0.383 mmol) in benzene (2.0 mL). The mixture was stirred for 2 h, and then the volatiles were evaporated and the crude product was slurried in hexane (10 mL). The solid was separated by filtration and dried *in vacuo* to yield a yellow powder (379 mg, 97%). Anal. Found: C, 58.88; H, 4.78; S, 6.01; Calcd for $C_{21}H_{16}Cl_2S_2O_2Rh_2$: C, 58.77; H, 4.73; S, 6.28. NMR spectra indicate the presence of *syn* and *anti* isomers in a ratio of approximately 1/3. ^{1}H NMR (400 MHz, CD_2Cl_2): δ 8.56 (d, $J_{H,H}$ = 4 Hz, 2H, Ar*H*, major isomer), 8.20 (d, $J_{H,H}$ = 8 Hz, 2H, Ar*H*, minor isomer), 7.26−6.44 (m, 26H, Ar*H*, major isomer), 7.26−6.44 (m, 26H, Ar*H*, minor isomer), 5.16 (s, 2H, S-C*H*R$_2$, minor isomer), 5.08 (s, 2H, S-C*H*R$_2$, major isomer), 1.20 (s, 18H, C(CH_3)$_3$, minor isomer), 1.04 (s, 18H, C(CH_3)$_3$, major isomer) ppm. ^{13}C NMR (400 MHz, CD_2Cl_2): δ

https://dx.doi.org/10.1021/acs.organomet.0c00094
Organometallics XXXX, XXX, XXX−XXX

146.31, 146.18, 139.91, 139.62, 138.91, 136.10, 136.00, 134.35, 131.57, 131.30, 130.87, 129.38, 128.92, 128.12, 127.74, 127.59, 127.34, 127.34, 125.65, 79.83, 78.00, 71.92, 71.45, 68.55, 63.04, 62.00, 26.39, 26.41 ppm. X-ray diffraction quality single crystals were grown from a filtered THF solution of the complex, which had been layered with pentane.

[(S_S,R_C)-10)RhCl]$_2$ ((R,R)-12). A solution of (S_S,R_C)-**10** (400 mg, 1.07 mmol) in benzene (4.0 mL) was added dropwise to a stirred solution of [RhCl(COE)$_2$]$_2$ (385 mg, 0.537 mmol) in benzene (4.0 mL), and the mixture was stirred overnight. After the solvent was removed under reduced pressure, the residue was slurried in pentane (15 mL), filtered, and vacuum-dried to afford a red-orange powder (566 mg, 97%). Anal. Found: C, 58.84; H, 4.85; S, 6.04. Calcd for $C_{21}H_{16}Cl_2S_2O_2Rh_2$: C, 58.77; H, 4.73; S, 6.28. ^{1}H NMR (270 MHz, benzene-d_6): δ 8.18 (d, $J_{H,H}$ = 7.8 Hz, 2H, ArH), 7.62 (d, $J_{H,H}$ = 7.8 Hz, 2H, ArH), 7.44−6.80 (m, 24H, ArH), 5.38 (s, 2H, S-CHR_2), 1.19 (s, 18H, C(CH_3)$_3$) ppm. X-ray diffraction quality single crystals were grown from a saturated and filtered benzene solution of the complex.

General Procedure for the Asymmetric Hayashi−Miyaura Reaction. In an inert-gas glovebox, a capped 20 mL vial with a magnetic stir bar was charged with 1.0 equiv of the enone, 2.0 equiv of boronic acid, and 0.03 equiv of either catalyst **11** or **12**. The reactions were performed on a 1−2 mmol scale. 1,4-Dioxane (3.0−6.0 mL) was added, and the reaction mixture was stirred for 30 min at 40 °C. A 0.5 equiv portion of aqueous Cs_2CO_3 (1.0 M, 0.5−1.0 mL) was added by syringe and the reaction mixture stirred for 24−28 h at 40 °C. Aqueous workup was performed by the addition of H_2O (5−10 mL) and EtOAc (5−10 mL). The phases were separated, and the aqueous phase was further extracted with EtOAc (3 × 15 mL). The combined organic phases were washed with brine (20 mL), dried over $MgSO_4$, filtered, and evaporated to dryness. The crude products, obtained as colorless or pale yellow oils or as white or off-white solids, were impregnated on silica G60 and purified by flash chromatography using *n*-hexane/EtOAc in varying ratios as eluent. This procedure affords practically quantitative isolated yields (>95%). Enantioenriched products **16aa**−**16ai**, **16ba**−**16be**, **16bg**−**16bi**, **16ca**, **16cb**, and **16cf**−**16ci** have been previously reported. For references, pertinent HPLC traces, and a general protocol for the synthesis of racemic reference substances, see the Supporting Information.

*3-(3-Methoxyphenyl)cyclopentan-1-one (**16bf**).* The general procedure outlined above was followed using catalyst **12** and 1.08 mmol of 2-cyclopenten-1-one. Purification by flash chromatography (hexane/EtOAc 9/1) afforded a colorless oil (202 mg, 98%). NMR spectroscopic data correspond to the racemic reference substance (see the Supporting Information). HPLC (Chiracel AS-H column, hexane/*i*PrOH 99/1, 0.6 mLmin^{-1}): ee = 96%, t_{R1} = 65.71 min, t_{R2} = 69.98 min (major).

*4-(4-(tert-Butyl)phenyl)tetrahydro-2H-pyran-2-one (**16cc**).* The general procedure outlined above was followed using catalyst **12** and 0.94 mmol of 5,6-dihydro-2*H*-pyran-2-one. Purification by flash chromatography (hexane/EtOAc 2/1) afforded a yellowish oil that slowly solidified at 0 °C (218 mg, 99%). NMR spectroscopic data correspond to the reference substance (see the Supporting Information). HPLC (Daicel Chiralpak AD-H column, hexane/*i*PrOH 95/5, 0.7 mL min^{-1}): ee = 97%, t_{R1} = 16.28 min (major), t_{R2} = 17.24 min.

*4-(4-Fluorophenyl)tetrahydro-2H-pyran-2-one (**16cd**).* The general procedure outlined above was followed using catalyst **12** and 1.06 mmol of 5,6-dihydro-2*H*-pyran-2-one. Purification by flash chromatography (hexane/EtOAc 2/1) afforded a colorless oil that slowly solidified (196 mg, 95%). NMR spectroscopic data correspond to the racemic reference substance (see the Supporting Information). HPLC (Daicel Chiralpak AS-H column, hexane/*i*PrOH 8/2, 1.0 mL min^{-1}): ee = 94%, t_{R1} = 25.28 min, t_{R2} = 27.47 min (major).

*4-(4-Methoxyphenyl)tetrahydro-2H-pyran-2-one (**16ce**).* The general procedure outlined above was followed using catalyst **12** and 1.03 mmol of 5,6-dihydro-2*H*-pyran-2-one. Purification by flash chromatography (hexane/EtOAc 2/1) afforded a colorless oil that solidified on prolonged standing (203 mg, 95%). NMR spectroscopic data correspond to the racemic reference substance (see the Supporting Information). HPLC (Daicel Chiralpak AS-H column, hexane/*i*PrOH 6/4, 0.7 mLmin^{-1}): ee = 94%, t_{R1} = 35.80 min, t_{R2} = 44.94 min (major).

Crystallographic Information. CCDC-1965291 for *rac*-**8**, CCDC-1965292 for (R_S,R_C)-**9**, CCDC-1965293 for (S_S,S_C)-**9**, CCDC-1965294 for (S_S,R_C)-**10**, CCDC-1965295 for (R,S)-**11**, and CCDC-1965296 for (R,R)-**12** contain supplementary crystallographic data for this paper. The data can be obtained free of charge from Cambridge Crystallographic Data Centre, 12 Union Road, Cambridge, CB2 1EZ, UK (fax: +44-1223-336-033; e-mail: deposit@ccdc.cam.ac.uk).

Intensity data of **8** were collected using Cu Kα radiation (λ = 1.54184 Å) on an Oxford Diffraction SuperNova dual radiation diffractometer with mirror optics. Intensity data of single crystals of the other compounds were collected using Mo Kα radiation (λ = 0.71073 Å) on either a Bruker Smart APEX 2 diffractometer (curved graphite monochromator) for (R_S,R_C)-**9** and (S_S,S_C)-**9** or a Bruker Kappa APEX 2 *IμS* Duo diffractometer equipped with QUAZAR focusing Montel optics for (S_S,R_C)-**10**, (R,S)-**11**, and (R,R)-**12**. Data were corrected for Lorentz and polarization effects, and semiempirical absorption corrections were performed on the basis of multiple scans using SADABS.[41] The structures were solved by direct methods (SHELX XT 2014/5)[42] and refined by full-matrix least-squares procedures on F^2 using SHELXL 2016/6.[43] All non-hydrogen atoms were refined with anisotropic displacement parameters. All hydrogen atoms were placed in positions of optimized geometry, and their isotropic displacement parameters were tied to those of the corresponding carrier atoms by a factor of either 1.2 or 1.5. Compound (R,S)-**11** crystallized with four molecules of tetrahydrofuran in its asymmetric unit. In (R,R)-**12** the complex molecule was situated on a crystallographic 2-fold rotation axis. This compound crystallized with a total of seven molecules of benzene per formula unit. Three out of the five independent benzene molecules were situated on crystallographic 2-fold rotation axes. Similarity restraints were applied to the anisotropic displacement parameters of the atoms of some solvent molecules. Pseudoisotropic restraints were applied to the anisotropic displacement parameters of all carbon atoms. The overall crystal quality was rather poor. There were two significant residual electron density maxima observed. These were attributed to truncation effects, as they could not be attributed to any disorder. There were also no signs of twinning (see also *K* value statistics).

Olex2 was used to prepare material for publication.[44] Crystallographic data, data collection, and structure refinement details are given in Table S1 in the Supporting Information.

Computational Details. Geometries were optimized with the Gaussian09 package using the PBE0-D$_3$ functional. The electronic configuration of the system was described with the split-valence SVP basis set for main-group atoms (C, H, S, and O) and the relativistic Stuttgart−Dresden effective core potential with the associated valence triple-ζ basis set for Rh. All geometries were confirmed as a minimum or transition state through frequency calculations. The reported free energies were built through single-point energy calculations on the PBE0-D3 geometries using the PBE0-D3 functional and the triple-ζ TZVP basis set for main-group atoms. Solvent effects were included with the PCM model using 1,4-dioxane as the solvent. To this PBE0-D3/TZVP electronic energy in solvent were added thermal corrections from the gas-phase frequency calculations at the PBE0-D3/SVP level.

■ ASSOCIATED CONTENT

Supporting Information

The Supporting Information is available free of charge at https://pubs.acs.org/doi/10.1021/acs.organomet.0c00094.

NMR spectra of ligands, complexes, and catalysis products, ORTEP of (S_S,S_C)-**9**, HPLC traces of ligands and catalysis products, and synthetic procedures for racemic reference substances (PDF)

Cartesian coordinates for the calculated structures (XYZ)

https://dx.doi.org/10.1021/acs.organomet.0c00094
Organometallics XXXX, XXX, XXX−XXX

Accession Codes

CCDC 1965291−1965296 contain the supplementary crystallographic data for this paper. These data can be obtained free of charge via www.ccdc.cam.ac.uk/data_request/cif, or by emailing data_request@ccdc.cam.ac.uk, or by contacting The Cambridge Crystallographic Data Centre, 12 Union Road, Cambridge CB2 1EZ, UK; fax: +44 1223 336033.

AUTHOR INFORMATION

Corresponding Authors

Ahmed Chelouan − *Department Chemie und Pharmazie, Anorganische und Allgemeine Chemie, Friedrich-Alexander-Universität Erlangen-Nürnberg, 91058 Erlangen, Germany*; Email: ahmed.chelouan@fau.de

Romano Dorta − *Department Chemie und Pharmazie, Anorganische und Allgemeine Chemie, Friedrich-Alexander-Universität Erlangen-Nürnberg, 91058 Erlangen, Germany*; orcid.org/0000-0001-5986-9729; Email: romano.dorta@fau.de

Authors

Alexander Nikol − *Department Chemie und Pharmazie, Anorganische und Allgemeine Chemie, Friedrich-Alexander-Universität Erlangen-Nürnberg, 91058 Erlangen, Germany*

Ziyun Zhang − *Catalysis Research Center, Physical Sciences and Engineering Division, King Abdullah University of Science and Technology, Thuwal, Saudi Arabia*

Laura Falivene − *Catalysis Research Center, Physical Sciences and Engineering Division, King Abdullah University of Science and Technology, Thuwal, Saudi Arabia*; orcid.org/0000-0003-1509-6191

Luigi Cavallo − *Catalysis Research Center, Physical Sciences and Engineering Division, King Abdullah University of Science and Technology, Thuwal, Saudi Arabia*; orcid.org/0000-0002-1398-338X

Alberto Herrera − *Department Chemie und Pharmazie, Anorganische und Allgemeine Chemie, Friedrich-Alexander-Universität Erlangen-Nürnberg, 91058 Erlangen, Germany*

Frank W. Heinemann − *Department Chemie und Pharmazie, Anorganische und Allgemeine Chemie, Friedrich-Alexander-Universität Erlangen-Nürnberg, 91058 Erlangen, Germany*; orcid.org/0000-0002-9007-8404

Ana Escalona − *Department Chemie und Pharmazie, Anorganische und Allgemeine Chemie, Friedrich-Alexander-Universität Erlangen-Nürnberg, 91058 Erlangen, Germany*

Sibylle Frieß − *Department Chemie und Pharmazie, Anorganische und Allgemeine Chemie, Friedrich-Alexander-Universität Erlangen-Nürnberg, 91058 Erlangen, Germany*

Alexander Grasruck − *Department Chemie und Pharmazie, Anorganische und Allgemeine Chemie, Friedrich-Alexander-Universität Erlangen-Nürnberg, 91058 Erlangen, Germany*

Complete contact information is available at: https://pubs.acs.org/10.1021/acs.organomet.0c00094

Notes

The authors declare no competing financial interest.

ACKNOWLEDGMENTS

We thank Prof. Anthony Linden (University of Zurich) for solving the crystal structure of **8** and Ms. Christina Wronna for carrying out the elemental analyses. Financial support by Friedrich−Alexander University and King Abdullah University of Science and Technology (KAUST) is acknowledged. For computer time, this research used the resources of the Supercomputing Laboratory (KSL) at KAUST.

REFERENCES

(1) *Ligand Design in Metal Chemistry, Reactivity and Catalysis*; Stradiotto, M., Lundgren, R. J., Eds.; Wiley: 2016.

(2) [5*H*]-dibenz[*b*,*f*]azepine is an inexpensive building block for the synthesis of essential medicines, such as carbamazepine. For its use in chiral ligands, see: (a) Defieber, C.; Ariger, M. A.; Moriel, P.; Carreira, E. M. Iridium-Catalyzed Synthesis of Primary Allylic Amines from Allylic Alcohols: Sulfamic Acid as Ammonia Equivalent. *Angew. Chem., Int. Ed.* **2007**, *46*, 3139−3143. (b) Briceño, A.; Dorta, R. *cis*-Dichloridobis{[(*S*)-N-(3,5-dioxa-4-phosphacyclohepta[2,1-a;3,4-a′]-dinaphthalen-4-yl]dibenz[*b*,*f*]azepin-κ*P*}-palladium(II) deuterochloroform disolvate. *Acta Crystallogr.* **2007**, *E63*, m1718−m1719. (c) Mariz, R.; Briceño, A.; Dorta, R.; Dorta, R. Chiral Dibenzazepine-Based P-Alkene Ligands and Their Rhodium Complexes: Catalytic Asymmetric 1,4 Additions to Enones. *Organometallics* **2008**, *27*, 6605−6613. (d) Herrera, A.; Linden, A.; Heinemann, F.; Brachvogel, R.-C.; von Delius, M.; Dorta, R. Optimized Syntheses of Optically Pure P-Alkene Ligands; Crystal Structures of a Pair of P-Stereogenic Diastereomers. *Synthesis* **2016**, *48*, 1117−1123. (e) Herrera, A.; Grasruck, A.; Heinemann, F. W.; Scheurer, A.; Chelouan, A.; Frieß, S.; Seidel, F.; Dorta, R. Developing P-Stereogenic, Planar-Chiral P-Alkene Ligands: Monodentate, Bidentate, and Double Agostic Coordination Modes on Ru(II). *Organometallics* **2017**, *36*, 714−720.

(3) For crystallographically authenticated ligand hemilability, see: (a) Reference 4. (b) Linden, A.; Llovera, L.; Herrera, J.; Dorta, R.; Agrifoglio, G.; Dorta, R. Chiral-at-Metal" Hemilabile Nickel Complexes with a Latent d^{10}-ML_2 Configuration: Receiving Substrates with Open Arms. *Organometallics* **2012**, *31*, 6162−6171.

(4) Drinkel, E.; Briceño, A.; Dorta, R.; Dorta, R. Hemilabile P-Alkene Ligands in Chiral Rhodium and Copper Complexes: Catalytic Asymmetric 1,4 Additions to Enones. 2. *Organometallics* **2010**, *29*, 2503−2514. The hemilability of **1** appears to be operative also in the Rh-catalyzed asymmetric Pauson−Khand reaction: (c) Burrows, L. C.; Jesikiewicz, L. T.; Lu, G.; Geib, S. J.; Liu, P.; Brummond, K. M. Computationally Guided Catalyst Design in the Type I Dynamic Kinetic Asymmetric Pauson−Khand Reaction of Allenyl Acetates. *J. Am. Chem. Soc.* **2017**, *139*, 15022.

(5) (a) Rössler, S. L.; Krautwald, S.; Carreira, E. M. Study of Intermediates in Iridium−(Phosphoramidite,Olefin)-Catalyzed Enantioselective Allylic Substitution. *J. Am. Chem. Soc.* **2017**, *139*, 3603−3606. (b) For the synthesis and crystal structure of $[Ir(\mathbf{1})_2Cl]$, see:. (c) Linden, A.; Dorta, R. *Acta Crystallogr., Sect. C: Cryst. Struct. Commun.* **2010**, *C66*, m290.

(6) (a) Hayashi, T.; Ueyama, K.; Tokunaga, N.; Yoshida, K. A Chiral Chelating Diene as a New Type of Chiral Ligand for Transition Metal Catalysts: Its Preparation and Use for the Rhodium-Catalyzed Asymmetric 1,4-Addition. *J. Am. Chem. Soc.* **2003**, *125*, 11508. (b) Defieber, C.; Paquin, J.-F.; Serna, S.; Carreira, E. M. Chiral [2.2.2] Dienes as Ligands for Rh(I) in Conjugate Additions of Boronic Acids to a Wide Range of Acceptors. *Org. Lett.* **2004**, *6*, 3873−3876. (c) Paquin, J. F.; Stephenson, C. R. J.; Defieber, C.; Carreira, E. M. Catalytic Asymmetric Synthesis with Rh-Diene Complexes: 1,4-Addition of Arylboronic Acids to Unsaturated Esters. *Org. Lett.* **2005**, *7*, 3821−3824. (d) Paquin, J.-F.; Defieber, C.; Stephenson, C. R. J.; Carreira, E. M. Asymmetric Synthesis of 3,3-Diarylpropanals with Chiral Diene-Rhodium Catalysts. *J. Am. Chem. Soc.* **2005**, *127*, 10850. (e) Otomaru, Y.; Okamoto, K.; Shintani, R.; Hayashi, T. Preparation of C_2-Symmetric Bicyclo[2.2.2]octa-2,5-diene Ligands and Their Use for Rhodium-Catalyzed Asymmetric 1,4-Addition of Arylboronic Acids. *J. Org. Chem.* **2005**, *70*, 2503−2508. (f) Wang, Z.-Q.; Feng, C.-G.; Xu, M.-H.; Lin, G.-Q. Design of C_2-Symmetric Tetrahydropentalenes as New Chiral Diene Ligands for Highly Enantioselective Rh-Catalyzed Arylation of N-Tosylarylimines with Arylboronic Acids. *J. Am. Chem. Soc.* **2007**, *129*, 5336−5337. (g) Melcher, M.-C.; Ivsic, T.; Olagnon, C.; Tenten, C.; Lützen, A.; Strand, D. Control of Enantioselectivity in Rhodium(I) Catalysis by Planar Chiral Dibenzo[*a*,*e*]-

cyclooctatetraenes. *Chem. - Eur. J.* **2018**, *24*, 2344−2348. (h) Melcher, M.-C.; Alves da Silva, B. R.; Ivšic, T.; Strand, D. Chiral Discrimination in Rhodium(I) Catalysis by 2,5 Disubstituted 1,3a,4,6a-Tetrahydropentalene Ligands−More Than Just a Twist of the Olefins? *ACS Omega* **2018**, *3*, 3622−3630.

(7) (a) Trost, B. M.; Rao, M. Development of Chiral Sulfoxide Ligands for Asymmetric Catalysis. *Angew. Chem., Int. Ed.* **2015**, *54*, 5026. (b) Sipos, G.; Drinkel, E.; Dorta, R. The emergence of sulfoxides as efficient ligands in transition metal catalysis. *Chem. Soc. Rev.* **2015**, *44*, 3834−3860. (c) Otocka, S.; Kwiatkowska, M.; Madalinska, L.; Kielbasinski, P. Chiral Organosulfur Ligands/Catalysts with a Stereogenic Sulfur Atom: Applications in Asymmetric Synthesis. *Chem. Rev.* **2017**, *117*, 4147−4181.

(8) For reviews on S(O)-alkene ligands, see: (a) Dong, H.-Q; Xu, M.-H.; Feng, C.-G.; Sun, X.-W.; Lin, G.-Q. Recent applications of chiral N-*tert*-butanesulfinyl imines, chiral diene ligands and chiral sulfur−olefin ligands in asymmetric synthesis. *Org. Chem. Front.* **2015**, *2*, 73. (b) Li, Y.; Xu, M.-H. Simple sulfur−olefins as new promising chiral ligands for asymmetric catalysis. *Chem. Commun.* **2014**, *50*, 3771. (c) Feng, X.; Du, H. Synthesis of Chiral Olefin Ligands and their Application in Asymmetric Catalysis. *Asian J. Org. Chem.* **2012**, *1*, 204.

(9) (a) Sakai, M.; Hayashi, H.; Miyaura, N. Rhodium-Catalyzed Conjugate Addition of Aryl- or 1-Alkenylboronic Acids to Enones. *Organometallics* **1997**, *16*, 4229−4231. (b) Takaya, Y.; Ogasawara, M.; Hayashi, T.; Sakai, M.; Miyaura, M. Rhodium-Catalyzed Asymmetric 1,4-Addition of Aryl- and Alkenylboronic Acids to Enones. *J. Am. Chem. Soc.* **1998**, *120*, 5579−5580. (c) Takaya, Y.; Ogasawara, M.; Hayashi, T. Asymmetric 1,4-Addition of Phenylboronic Acid to 2-Cyclohexenone Catalyzed by Rh(I)/binap Complexes. *Chirality* **2000**, *12*, 469.

(10) Poater, A.; Ragone, F.; Mariz, R.; Dorta, R.; Cavallo, L. Comparing the Enantioselective Power of Steric and Electrostatic Effects in Transition-Metal-Catalyzed Asymmetric Synthesis. *Chem. - Eur. J.* **2010**, *16*, 14348−14353.

(11) The diastereomer of **3** is also readily accessible: Thaler, T.; Guo, L.-N.; Steib, A. K.; Raducan, M.; Karaghiosoff, K.; Mayer, P.; Knochel, P. Sulfoxide_Alkene Hybrids: A New Class of Chiral Ligands for the Hayashi−Miyaura Reaction. *Org. Lett.* **2011**, *13*, 3182−3185.

(12) (a) Chen, G.; Giu, J.; Li, L.; Liao, J. Chiral Sulfoxide-Olefin Ligands: Completely Switchable Stereoselectivity. *Angew. Chem., Int. Ed.* **2011**, *50*, 7681. For ligand synthesis, see also: (b) Xue, F.; Li, X.; Wan, B. A Class of Benzene Backbone-Based Olefin−Sulfoxide Ligands for Rh-Catalyzed Enantioselective Addition of Arylboronic Acids to Enones in Rhodium-Catalyzed Asymmetric Conjugate Additions. *J. Org. Chem.* **2011**, *76*, 7256.

(13) Chelouan, A.; Bao, S.; Frieß, S.; Herrera, A.; Heinemann, F.; Escalona, A.; Grasruck, A.; Dorta, R. Developing Chiral Dibenzazepine-based S(O)-Alkene Hybrid Ligands for Rh(I) Complexation: Catalysts for the Base-Free Hayashi Miyaura Reaction. *Organometallics* **2018**, *37*, 3983.

(14) For example, sulfinylamines can be attacked by strong nucleophiles, such as Grignards, to form sulfoxides: Gais, H.-J.; Reddy, L. R.; Babu, G. S.; Raabe, G. Asymmetric Synthesis of 2,3-Dihydrofurans and of Unsaturated Bicyclic Tetrahydrofurans through α-Elimination and Migratory Cyclization of Silyloxy Alkenyl Aminosulfoxonium Salts. Generation and Intramolecular O,Si-Bond Insertion of Chiral Disubstituted □-Silyloxy Alkylidene Carbenes. *J. Am. Chem. Soc.* **2004**, *126*, 4859.

(15) For the use of the phenyl-dibenzotropylidenyl moiety in a chiral phosphine ligand, see: Piras, E.; Läng, F.; Rüegger, H.; Stein, D.; Wörle, M.; Grützmacher, H. Chiral Phosphane Alkenes (PALs): Simple Synthesis, Applications in Catalysis, and Functional Hemilability. *Chem. - Eur. J.* **2006**, *12*, 5849−5858.

(16) "Matched" means that various stereocenters in the ligand/metal catalyst synergistically favor the formation of the same product enantiomer. For an excellent introductory review, see: (a) Doyle, M. P.; Morgan, J. P.; Fettinger, J. C.; Zavalij, P. Y.; Colyer, J. T.; Timmons, D. J.; Carducci, M. D. Matched/Mismatched" Diastereomeric Dirhodium(II) Carboxamidate Catalyst Pairs. Structure-Selectivity Correlations in Diazo Decomposition and Hetero-Diels-Alder Reactions. *J. Org. Chem.* **2005**, *70*, 5291−5301. The same principle may also apply for combinations of chiral heteroligands: (b) Monti, C.; Gennari, C.; Piarulli, U. Rh-Catalyzed Enantioselective Conjugate Addition of Arylboronic Acids with a Dynamic Library of Chiral tropos Phosphorus Ligands. *Chem. - Eur. J.* **2007**, *13*, 1547−58.

(17) (a) Colonge, J.; Sibeud, J.; Boisdk, P. *Bull. Soc. Chim. Fr.* **1953**, 767. (b) Tardieu, P. Déshydratation des alcools mésodhydroanthracéniques primaires et secondaires. *Ann. Chim. (Paris)* **1961**, *6*, 1445. (c) Knorr, R.; Lattke, E.; Räpple, E. Der konformative *ortho*-Effekt bei *o*-Tolylstilbenen und deren Vinyllithiumderivaten. *Chem. Ber.* **1981**, *114*, 1581−92.

(18) Deblon, S.; Ruegger, H.; Schonberg, H.; Loss, S.; Gramlich, V.; Grützmacher, H. Highly distorted d^8-rhodium(+I) and d^{10}-rhodium-(−I) complexes: synthesis, reactivity, and structures in solution and solid state. *New J. Chem.* **2001**, *25*, 83−92.

(19) Añez, R.; Calderón, J.; Herrera, A.; Linden, A.; Dorta, R. Manuscript in preparation. The behavior of **8** in solution at low temperature is currently being investigated in our laboratory. For a related helical system that is stable at RT, see: Chung, J.-Y.; Schulz, C.; Bauer, H.; Sun, Y.; Sitzmann, H.; Auerbach, H.; Pierik, A. J.; Schünemann, V.; Neuba, A.; Thiel, W. R. Cyclopentadienide Ligand Cp^{C-} Possessing Intrinsic Helical Chirality and Its Ferrocene Analogues. *Organometallics* **2015**, *34*, 5374−5382.

(20) The racemate also serves as ra eference substance for HPLC certification of the stereochemical purity of the optically active ligands.

(21) LDA/*t*-BuOK turned out to be the base of choice, giving higher enantioselectivities and yields in comparison to the preformed and isolated Li- and K-tropylidenides.

(22) (a) Llera, J. M.; Fernández, I.; Alcudia, F. An efficient synthesis of both enantiomers of chiral non racemic methylsulfoxides from DAG. *Tetrahedron Lett.* **1991**, *32*, 7299. (b) Fernández, I.; Khiar, N.; Llera, J. M.; Alcudia, F. Asymmetric Synthesis of Alkane- and Arenesulfinates of Diacetone-D-glucose (DAG): An Improved and General Route to Both Enantiomerically Pure Sulfoxides. *J. Org. Chem.* **1992**, *57*, 6789. (c) Khiar, N.; Fernández, I.; Alcudia, F. Asymmetric synthesis of optically pure *tert*-butyl sulfoxides using the "DAG methodology. *Tetrahedron Lett.* **1994**, *35*, 5719−5722. For the first DAG-derived sulfinates, see: (d) Ridley, D. D.; Smal, M. A. Use of Carbohydrates in the Preparation of Optically Active Sulfoxides. *J. Chem. Soc., Chem. Commun.* **1981**, 505. (e) Ridley, D. D.; Smal, M. A. Preparation of Arenesulfinic Esters of 1,2:5,6-Di-0-cyclohexylidene-α-D-glucofuranose, and Their Conversion into Optically Active Sulfoxides. *Aust. J. Chem.* **1982**, *35*, 495. For the structural characterization of **11**, see ref 13.

(23) For mechanistic considerations regarding the stereospecificity of lithium C-nucleophiles with Andersen's sulfinate, see: Rayner, P. J.; O'Brien, P.; Horan, R. A. J. Preparation and Reactions of Enantiomerically Pure α-Functionalized Grignard Reagents. *J. Am. Chem. Soc.* **2013**, *135*, 8071−8077.

(24) The high solubility difference of the two diastereomers in EtOAc makes their separation by crystallization a viable option, especially on larger scales.

(25) The reaction conditions were not optimized (work in progress).

(26) Structurally authenticated chiral S(O)-alkene complexes of Rh are quite rare. See refs 11 and 12a and: Feng, X.; Wang, Y.; Wei, B.; Yang, J.; Du, H. Simple *N*-Sulfinyl-Based Chiral Sulfur-Olefin Ligands for Rhodium-Catalyzed Asymmetric 1,4-Additions. *Org. Lett.* **2011**, *13*, 3300−3303.

(27) (a) Dewar, M. J. S. A review of π Complex Theory. *Bull. Chem. Soc. Fr.* **1951**, *18*, C71−79. (b) Chatt, J.; Duncanson, L. A. Olefin Coordination Compounds. Part III. Infra-red Spectra and Structure: Attempted Preparation of Acetylene Complexes. *J. Chem. Soc.* **1953**, 2939.

(28) (i) Reactions in toluene are slower and less selective. (ii) A base additive improves activity and selectivity in the following order: KOH < KF < $K_3PO_4 \approx Cs_2CO_3$. (iii) Catalyst loadings of <1.5 mol % cause erosion of enantioselectivity.

(29) Hayashi, T.; Takahashi, M.; Takaya, Y.; Ogasawara, M. Catalytic Cycle of Rhodium-Catalyzed Asymmetric 1,4-Addition of Organo-

https://dx.doi.org/10.1021/acs.organomet.0c00094
Organometallics XXXX, XXX, XXX−XXX

boronic Acids. Arylrhodium, Oxa-π-allylrhodium, and Hydroxorhodium Intermediates. *J. Am. Chem. Soc.* **2002**, *124*, 5052−5058.
(30) For similar stereochemical models featuring S(O)-alkene ligands, see refs 11 and 12a and: Chen, Q.; Chen, C.; Guo, F.; Xia, W. Application of chiral *N-tert*-butylsulfinyl vinyl aziridines in Rh(I) catalyzed 1,4-addition of aryl boronic acids to cyclic enones. *Chem. Commun.* **2013**, *49*, 6433−6435.
(31) (a) Falivene, L.; Credendino, R.; Poater, A.; Petta, A.; Serra, L.; Oliva, R.; Scarano, V.; Cavallo, L. SambVca 2. A Web Tool for Analyzing Catalytic Pockets with Topographic Steric Maps. *Organometallics* **2016**, *35*, 2286−2293. (b) Falivene, L.; Cao, Z.; Petta, A.; Serra, L.; Poater, A.; Oliva, R.; Scarano, V.; Cavallo, L. Towards the online computer-aided design of catalytic pockets. *Nat. Chem.* **2019**, *11*, 872−879.
(32) The electrostatic maps show an inverted pattern and are less conclusive. See Figure S39 in the Supporting Information.
(33) Korenaga, T.; Maenishi, R.; Hayashi, K.; Sakai, T. Highly Active and Enantioselective Rhodium-Catalyzed Asymmetric 1,4-Addition of Arylboronic Acid to α,β-Unsaturated Ketone by using Electron-Poor MeO-F_{12}-BIPHEP. *Adv. Synth. Catal.* **2010**, *352*, 3247.
(34) (a) Chelouan, A.; Recio, R.; Alcudia, A.; Khiar, N.; Fernández, I. DMAP-Catalysed Sulfinylation of Diacetone-D-Glucose: Improved Method for the Synthesis of Enantiopure *tert*-Butyl Sulfoxides and *tert*-Butanesulfinamides. *Eur. J. Org. Chem.* **2014**, *2014*, 6935−6944. (b) Reference 13..
(35) Schlosser, M.; Ladenberger, V. Notiz über die Darstellung reiner Lithiumaryle. *J. Organomet. Chem.* **1967**, *8*, 193.
(36) Van der Ent, A.; Onderlinden, A. L.; Schunn, R. A. Chlorobis(cyclooctene)rhodium(I) and − iridium(I) complexes. *Inorg. Synth.* **2007**, *28*, 90.
(37) Matos, P. M.; Lewis, W.; Moore, J. C.; Stockman, R. A. Sulfonimidates: Useful Synthetic Intermediates for Sulfoximine Synthesis *via* C−S Bond Formation. *Org. Lett.* **2018**, *20*, 3674−3677.
(38) Fulmer, G. R.; Miller, A. J. M.; Sherden, N. H.; Gottlieb, H. E.; Nudelman, A.; Stoltz, B. M.; Bercaw, J. E.; Goldberg, K. I. NMR Chemical Shifts of Trace Impurities: Common Laboratory Solvents, Organics, and Gases in Deuterated Solvents Relevant to the Organometallic Chemist. *Organometallics* **2010**, *29*, 2176.
(39) *Delta NMR Processing and Control Software, ver. 4.3.6*; JEOL USA: Peabody, MA, USA, 1990−2006.
(40) Schmuck, C.; Wienand, W. The First Efficient Synthesis and Optical Resolution of Monosubstituted Cyclotribenzylenes. *Synthesis* **2002**, *2002*, 655−663.
(41) *SADABS 2014/5, Bruker AXS area detector scaling and absorption correction*; Bruker AXS: Madison, WI, USA, 2014.
(42) Sheldrick, G. M. A short history of SHELX. *Acta Crystallogr., Sect. A: Found. Crystallogr.* **2008**, *64*, 112.
(43) Sheldrick, G. M. (2015) Crystal structure refinement with SHELXL. *Acta Crystallogr., Sect. C: Struct. Chem.* **2015**, *71*, 3. (Open Access).
(44) Dolomanov, O. V.; Bourhis, L. J.; Gildea, R. J.; Howard, J. A. K; Puschmann, H. OLEX2: a complete structure solution, refinement and analysis program. *J. Appl. Crystallogr.* **2009**, *42*, 339.

https://dx.doi.org/10.1021/acs.organomet.0c00094
Organometallics XXXX, XXX, XXX−XXX